Latin American Journal of Solids and Structures
www.lajss.org

The Effectiveness of Thin-Walled Hull Structures Against Collision Impact

Abstract

The impact phenomenon is one of many subjects that is interesting and has become an inseparable part of naval architecture and ocean engineering fields. Limitless possibilities in cause and scenario make the demand to understand the physical behavior of ship structures due to impact phenomenon is increasing. In present work, a series of virtual experiment is performed by finite element method to solve several defined collision scenarios. Two involved ships are classified as the *striking ship* which penetrates the target and *struck ship* as the target. Hull arrangement of the struck ship is considered as main parameter which single and double hull configurations are proposed to be assessed. An observation of the damage extent on struck ship subjected to collision loads are presented. The results indicate that the internal arrangement of the struck ship provides significant effects to resistance capability and structural failure after collision process. Finally, an analysis regarding the extent of the damage is summarized with a statistical calculation to provide distribution of crashworthiness criteria of the defined scenarios.

Keywords

Impact phenomena, ship-ship collision; single and double hull structures; internal energy; damage extent.

Aditya Rio Prabowo [a]
Seung Jun Baek [b]
Hyun Jin Cho [b]
Jung Hoon Byeon [b]
Dong Myung Bae [b]
Jung Min Sohn [b]

[a] Interdisciplinary Program of Marine Convergence Design, Pukyong National University, South Korea
[b] Department of Naval Architecture and Marine Systems Engineering, Pukyong National University, South Korea
[jminz@pknu.ac.kr]

http://dx.doi.org/10.1590/1679-78253895

Received 04.04.2017
In revised form 15.05.2017
Accepted 15.05.2017
Available online 26.05.2017

1 INTRODUCTION

The role of the ship in human activity is very important, for example as a distributor of commodities, as well as for tourism and public transportation. The safety during sailing and distribution for these objectives is very important especially when subjected to an impact phenomena. The impact may possibly threat the ship, passengers and carried cargo which can make a loss unavoidably immense. Researchers paid their attention to massive environmental damage on accident of the *Exxon Valdez* in Alaska (Alsos and Amdahl, 2007) while development in assessment method is conducted until

computational calculation is introduced to calculate crash of various objects, such as ship (Kitamura, 2002), ice and steel (Bae et al., 2016) and seabed topology with bottom structure (AbuBakar and Dow, 2013). Development of estimation technology is found walk side by side with a growth of human population and interest to expand point of interest for tourist site. In this situation, demands of a ship as public transportation can be seen significantly in various archipelago countries. The use of the Roll on-Roll off (Ro-Ro) passenger ship holds a vital role in distributing and delivering industry products from one island to the other one, e.g. Indonesia, Ireland, New Zealand and Maldives as maritime countries. Ro-Ro is preferable than a cargo vessel or container ship because the cargo distribution can be continued by truck or mini truck to a specific city, town and even village when the carried commodities arrive at their destined port. Besides that, distribution of large amount of passenger and tourist is possible to be conducted with this ship. Considering the importance of the passenger ship in daily life and demand to ensure ship performance in experiencing impact phenomena, implementation of assessment method is seriously encouraged to calculate various impact scenarios.

The present research will focus on the structural integrity of a Ro-Ro passenger ship subjected to several collision scenarios. The impact configuration is defined as a contact between two ship structures which the struck ship is penetrated by the striking ship from side direction. Two different structural arrangements are proposed to be studied in order to obtain an adequate information regarding structural behaviour and estimation of structural crashworthiness of the struck ship under collision.

2 PIONEER RESEARCH AND RECENT OBSERVATION ON SHIP COLLISION

The design of construction, structure and any arrangement of materials can experience failure when subjected to various loads. In engineering, load is classified into many types which include periodic, constant and impact. Under periodic and constant loads, a structure undergoes failure when material of a structure cannot maintain the given loads that occur according to certain rhythm, e.g. periodic load of wave on a ship hull and constant load of container on a cargo hold in container ship. In the other hand, impact phenomena work with a very different concept compared to previous ones, regardless of the involved objects, such as train (Klinger and Bohraus, 2014), aircraft (James, 2002), or ship (Prabowo et al., 2016a-b). The impact possibly delivers fatal damage to local material and overall structure since it happens very fast and in several sources, it is known as short-period load. In the field of marine structures and ocean engineering, this load type usually occurs during maritime accidents, namely explosion, grounding and collision. In term of collision, it can occur due to an almost limitless variety of causes and scenarios, such as between ship and bridge, ship and frigate container and even between two ships. Wide range of possibility makes the capability of ship structure needs to be reviewed and analysed to ensure its safety, especially when subjected to certain impact load. As development of technology and concern to ship safety, impact phenomenon is observed and introduced by various methodologies. Minorsky (1958) performed a research based on the full-scale collision of various ships. This research produced an empirical formulae which was useful to estimate collision energy based on damage extent that occurred after collision. It also can be concluded that energy and damage in collision analysis are two important parameters of structural performance in the impact engineering field. A lot of effort was conducted to refine the Minorsky's formulae since it was consid-

ered only suitable for high-energy collisions. Twenty years after Minorsky, Woisin (1979) was successfully introducing a refined version of the previous formulae *so called low-energy formulae*. The improvement in empirical estimation and calculation was continuously performed, for instance by Vaughan (1978), Jones and Wierzbicki (1983) as well as Paik (1994) contributed to this field. The equations of Minorsky, Vaughan, as well as Jones and Wierzbicki are presented in Equation 1 to 3 consecutively.

$$E = 47.2R_T + 32.7 \tag{1}$$

$$E = \frac{1}{2} R_T \sigma_0 \left(\frac{2w}{l}\right)^2 \tag{2}$$

$$E = C_{1.5}.\sigma_0.l^{1.5}.t_{eq}{}^{1.5} \tag{3}$$

where E is absorbed energy, R_T is destroyed material volume for both struck and striking ship / resistance factor, H is height of rupture aperture in side shell, t_s is side shell thickness, A is area of tearing, σ_0 is the flow stress of the material, $2w / l$ is normalised finalised final deflection over the span, $C_{1.5}$ equals with $1.112 - 1.156\vartheta + 3.760\vartheta^2$ where ϑ is the half of the wedge t_{eq} is the equivalent plate thickness and ε_c is the critical rupture strain of the material which is determined from $\varepsilon_c = 0.10$ (ε_f / 0.32) where ε_f is the steel material ductility obtained in tensile test.

Different than empirical method, the analytical method is also considered good to calculate predicted casualties on structures due to impact load. This method works based on the upper bond theorem and some assumptions from observation of accidental damages and experimental studies. Usually, the methods can give good predictions through fast simple analysis. Therefore, many authors such as McDermott (1974), Kinkead (1980), Reckling (1983) as well as Wang and Ohtsubo (1997) have used the simplified analytical methods for analysis of ship collisions. A major assumption in this method is that different structural members such as the side shell, decks and frame, do not interact but contribute independently to the total resistance as presented by Zhang (1999). Analytical equations for deformation of side plating is given in Equations 4 and 5 while the deck is shown in Equations 6 and 7. Observation of mechanical behavior on structural member is also conducted recently by Zhang (2014) and Zahran (2017), while assessment of damage criterion accounting for various triaxial stresses is presented by Brünig et al. (2008).

$$E_p = \frac{1}{\sqrt{3}} \frac{4n^2}{4n^2 - 1} \sigma_0 t_p A\delta^2 \left(\frac{1}{a_1 a_2} + \frac{1}{b_1 b_2}\right) \tag{4}$$

$$F_p = \frac{2}{\sqrt{3}} \frac{4n^2}{4n^2 - 1} \sigma_0 t_p A\delta \left(\frac{1}{a_1 a_2} + \frac{1}{b_1 b_2}\right) \tag{5}$$

$$E_p = \frac{1}{\sqrt{3}} \frac{n^2}{4n^2 - 1} \sigma_0 t_p A\delta^2 \left(\frac{1}{a_1 a_2} + \frac{1}{(2b)^2}\right) \tag{6}$$

$$F_p = \frac{2}{\sqrt{3}} \frac{n^2}{4n^2 - 1} \sigma_0 t_p A\delta \left(\frac{1}{a_1 a_2} + \frac{1}{(2b)^2} \right. \tag{7}$$

where E_p is absorbed energy, F_p is resistance force, σ_0 is static flow stress, t_p is plate thickness, A is plate area, δ is indentation and a_1, a_2, b_1 and b_2 can be obtained in assumption for lateral area point analysis.

With the rapid development in computational equipment, the virtual experiment especially using the finite element method appears as a new and reliable assessment method. This method is judged powerful enough to calculate and predict various phenomena in science and engineering. Low cost if a failure occurs on experiment and large capability to analysis full-scale phenomena make this method is also applied to assess impact phenomena. Admittance regarding reliability of this method was proofed and stated by previous researchers namely Prabowo et al. (2017a) and Bae et al. (2016b) when they conducted a comparative study using numerical simulation, empirical method and observational data of an actual collision.

3 FUNDAMENTAL BASIS OF FAILURE FORMULATION

In performing assessments on material or structural capacity, failure becomes an important parameter to be discussed. It usually uses von Mises and Tresca contours to describe failure characteristic of a subject after various load types are applied on it. These contours are composed based on formulation. Firstly, the von Mises is representing a critical value of the distortional energy stored in the isotropic material while secondly, the Tresca is providing a critical value of the maximum shear stress in the isotropic material. Historically, the Tresca form was considered to be the more fundamental of the two, but the von Mises form was seen as an appealing and mathematically convenient approximation to it. In von Mises formulae, for maximum distortion or shear energy, yielding starts when the maximum distortion or shear energy in the material $W_{d,max}$ equals the maximum distortion or shear energy at yielding in a simple tension test $W_{d,y}$. Distortion or shear energy itself is part of the strain energy which corresponds to volume-preserved shape change. In term of the stress components, Equations 8 and 9 are given to describe $W_{d,max}$ and $W_{d,y}$ while the von Mises criterion is presented in Equations 10 and 11.

$$W_{d,\max} = \frac{1}{12G}\left[(\sigma_{xx} - \sigma_{yy})^2 + (\sigma_{yy} - \sigma_{zz})^2 + (\sigma_{zz} - \sigma_{xx})^2 + 6(\tau_{xy}{}^2 + \tau_{yz}{}^2 + \tau_{zx}{}^2)\right] \tag{8}$$

$$W_{d,\max} = \frac{1}{6G}\sigma_Y{}^2 \tag{9}$$

$$\frac{1}{\sqrt{2}}\left[(\sigma_{xx} - \sigma_{yy})^2 + (\sigma_{yy} - \sigma_{zz})^2 + (\sigma_{zz} - \sigma_{xx})^2 + 6(\tau_{xy}{}^2 + \tau_{yz}{}^2 + \tau_{zx}{}^2)\right]^{\frac{1}{2}} = \sigma_Y = \sigma_{vm} \tag{10}$$

$$\frac{1}{\sqrt{2}}\left[(\sigma_1 - \sigma_2)^2 + (\sigma_2 - \sigma_3)^2 + (\sigma_3 - \sigma_1)^2\right]^{\frac{1}{2}} = \sigma_Y = \sigma_{vm} \tag{11}$$

where $W_{d,max}$ is maximum distortion energy, $W_{d,y}$ is distortion energy in yield, G is shear modulus, σ_{xx}, σ_{yy} and σ_{zz} are normal stresses in 3-D plane, τ_{xy}, τ_{yz} and τ_{zx} are shear stress in 3-D plane, σ_1, σ_2 and σ_3 are principal stresses, σ_Y is yield stress and σ_{vm} is von Misses criterion.

As for the maximum shear stress of the Tresca formulae, yielding starts when the maximum shear stress in the material τ_{max} equals the maximum shear stress at yielding in a simple tension test τ_Y. This stress mathematically can be written as Equations 12 and 13 while the general form of Tresca criterion is given in Equation 14.

$$\tau_{\max} = \tau_Y \tag{12}$$

$$\tau_{\max} = \frac{\sigma_{\max} - \sigma_{\min}}{2} \tag{13}$$

$$\sigma_{\max} - \sigma_{\min} = \sigma_Y = \sigma_t \tag{14}$$

where τ_{max} is maximum shear stress, τ_y is shear stress in yielding, σ_{max} is maximum normal stress, σ_{min} is minimum normal stress, σ_Y is yield stress and σ_t is Tresca criterion.

4 ENGINEERING ANALYSIS

4.1 Collision Modelling

Impact simulations are performed for various penetration scenarios with the FE code ANSYS LS-DYNA (ANSYS, 2017). The struck ship was modelled as an idealized version of a real ship. Its particulars are as follows: a passenger ship, LOA 85 m, beam 16 m, GT 3898 t and DWT 683 t. In other hand, the striking ship is a 140 meters cargo reefer which is defined as a rigid body. Four target points with Points 1 and 2 on the double hull and Points 3 and 4 on the single hull are proposed to be used in the impact process as given in Figure 1a. The condition during collision process is defined by an analytical coordinate system which is built based on Cartesian coordinate system. As presented in Figure 1b, the striking ship is given velocity 10 knots or 5.14 m/s to move to the designated target points on the struck ship. The collision angle β is assumed to be perpendicular between the two ships.

4.2 Numerical Analysis

In side collision between the struck and striking ships, the struck ship as the target is set to be fixed in centerline while the ends of the model will be clamped. The fixation is applied on all frames and rotational displacement of longitudinal deck is restrained in the end model. Since a series of collision analysis is performed by numerical experiment, the mesh size must be large enough to obtain a practical simulation time, but sufficiently small to capture the major deformation modes. For the *main area* on the struck ship is defined between car deck and middle deck. In this area where the target points are determined, a meshing size with an approximation length 60 mm - 70 mm is applied. On the area with no significant deformation or stress gradients, larger meshing size of 120 - 480 mm is used. These sizes are calculated based on calculation of Prabowo et al (2017b-c) as well as recommendation of Tornqvist and Simonsen (2004) who suggested the element-length-to-thickness ratio should be within the range of 5-10 so that the local stress and strain fields can be captured well. The

deformable structure on the struck ship is embedded by the plastic-kinematics material. The yield characteristic of this material model is shown in Equation 15. In order to vary structural strength, several steels with different properties are used in analysis and given in Table 1. Kinematic hardening with constant $\beta = 0$, Cowper-Symonds strain parameter $c = 3200$ and $P = 5$ are appended to the properties. Tangent modulus is set to be higher than zero to avoid failure in convergence. It is recommended to obtain this property using tensile test. If it is not available $E_x/100$ can be considered to be implemented in analysis. Similar strategy to apply tangent modulus property and avoid zero value has been applied in previous work of Ozguc et al. (2005) during observation and investigation of structural integrity on bulk carrier.

$$\sigma_Y = \left[1 + \left(\frac{\varepsilon}{c}\right)^{\frac{1}{P}}\right]\left(\sigma_0 + \beta E_p \varepsilon_p^{\,eff}\right) \tag{15}$$

where σ_Y is yield stress, ε is strain rate, c is Cowper-Symonds strain rate parameters, P is Cowper - Symonds strain rate parameters, σ_o is initial yield stress, β is hardening parameter, E_p is plastic hardening modulus, and $\varepsilon_p^{\,eff}$ is effective plastic strain.

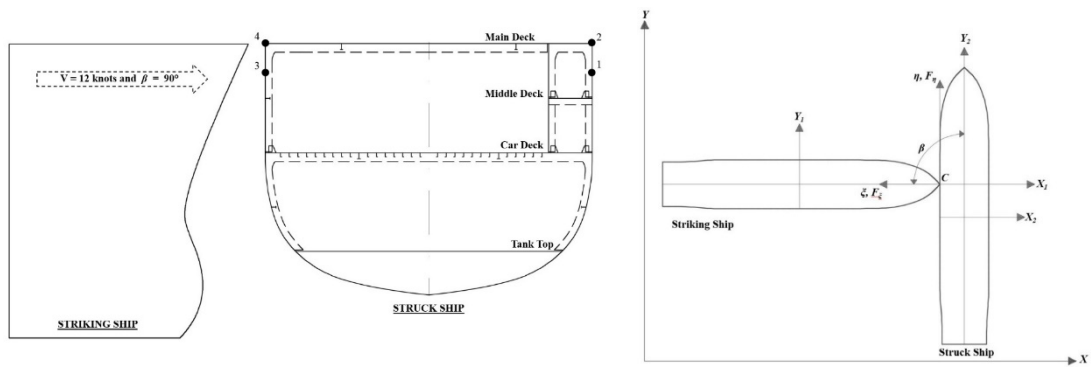

(a) (b)

Figure 1: Illustration of the defined collision scenarios. (a) The designated target point on the ship cross section. Right side represents double hull, and left side stands for single hull. (b) Coordinate system of the side collision between two ships.

Material No.	Density (kg/m^3)	M. Elasticity (MPa)	Yield S. (MPa)	Ultimate S. (MPa)	Poisson's Ratio
1	7,870	200,000	370	440	0.29
2	7,858	205,000	395	470	0.29
3	7,870	205,000	340	405	0.29
4	7,870	205,000	325	385	0.29

Table 1: Mechanical properties of marine steel for virtual experiment.

5 RESULTS AND DISCUSSION

5.1 Global Results of the Structural Crashworthiness

This section presents calculation results based on the defined parameters and scenarios in the previous sub-section. The collision energy on the struck ship is evaluated as the main subject and further observation is expanded into the damage extent in order to provide overall assessment on the crashworthiness criteria. The discussion is started from the collision energy. This energy is presented as a representative of the internal energy from numerical simulation, which indicates an amount of energy that is needed to plastically deform the involved objects in impact. The results indicated that the resistance on the single hull structure was bigger than on the double hull in term of collision to shell. During collisions that happened to the main deck for two structures, the main deck of the double sided structure was also proved to be more robust than the single hull. These tendencies are presented in Table 2 together with detail of damage characteristic on both outer and inner hull. Nevertheless, the according to the energy-damage relations such as presented by Minorsky (1958), Vaughan (1978), Woisin (1979) etc., collision energy should be perpendicular equal with the damage volume which consists accumulation of damage width, length and thickness of the destroyed part. If it is assumed that the thickness is constant along of the struck ship's hull, the collision energy is directly related to the damage length and width. It is observed that for collision to shell, the significance between two hull types is approximately 3 MJ which the double hull is superior to the single hull. However in damage assessment on the outer hull, the damage of two structures is not very different in term of the length and distinction in the width is less than 1 m.

Firstly, it can be concluded that the contribution of the inner hull after the outer hull was breached during side collision was found significant. The single hull structure which does not have the inner hull was evidenced produced less collision energy or it can be stated the resistance capability of the double hull is better against side penetration. This statement can be concluded as the collision energy is defined as the energy that is needed to make the structure and it material component exceed their yield capacity and undergo plastic deformation. Secondly, the contribution of the inner hull during the collision to deck is found very low and almost zero (Figures 2 and 3). Since the arrangements of the deck on the single and double structures are similar, the crashworthiness criteria in terms of collision energy and damage extent provide no significant difference. Even though the width on the double hull damage is smaller than single hull, resistance is provided with the inner hull which was displaced 0.74 m after collision. In other hand, the single hull produced wider tearing and similar collision energy with the double hull structure in the end of collision process.

5.2 Damage Extent on the Struck Ship

Under *collision to shell* scenario to the struck ship, the double hull structure experienced similar damage length as shown in Figure 4. The von Mises contour on the double hull indicated that expansion area of the stress occurred along the longitudinal members. On the upper side, the stress expanded along intercostal of the outer hull and deck. Meanwhile on the lower side, observation presented wide stress distribution on two locations, namely outer hull-middle deck and outer hull-car deck intercostals. On the single hull structure, the stress distribution was stopped on the transition structure before it reached after-end part. This phenomenon occurred as the longitudinal stringer on

the outer hull only existed on the single hull part. At the after-end location, a double hull arrangement was designed and dominated by transverse components. The distributions were observed on three locations that similar with the double hull structure. However, outer hull-middle deck intercostal was not found on the single hull structure and the outer hull was strengthened by longitudinal stiffener instead. Therefore, the stress distribution was found on outer hull-longitudinal stiffener intercostal of the single hull structure.

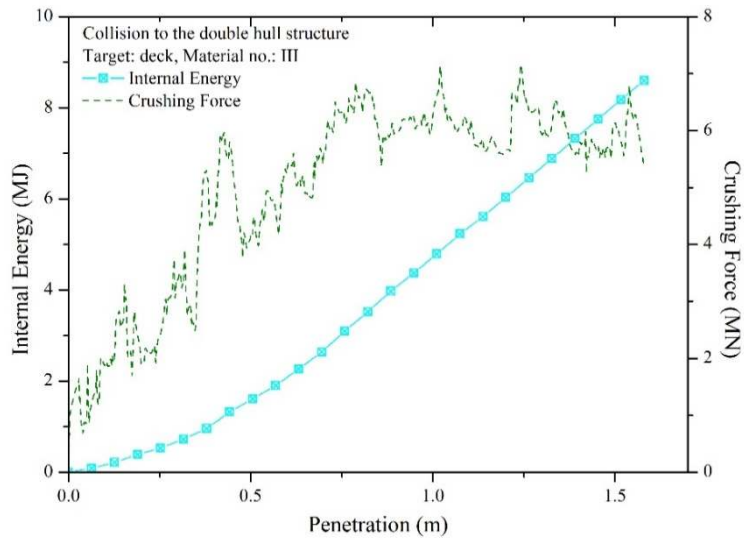

Figure 2: Energy and force behavior during collision on the double hull structure.

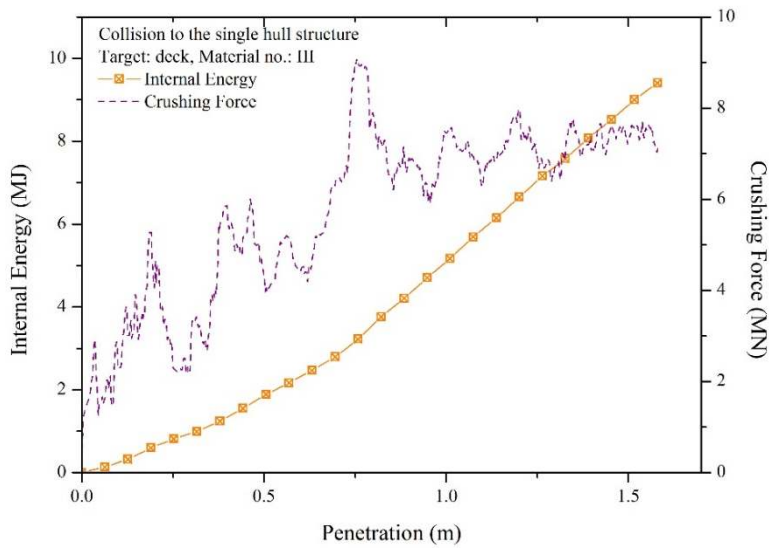

Figure 3: Energy and force behavior during collision on the single hull structure.

Construction Type	Target Location	Material No.*	Collision Energy (MJ)	Damage Extent				
				Outer Hull		Inner Hull		
				Length (m)	Width (m)	Length (m)	Width (m)	Displ.** (m)
Double Hull	Shell	I	9.0827	3.9350	2.4994	1.5833	0.1129	0.4996
		II	9.8800	3.8309	2.4787	1.4605	0.1037	0.4996
		III	8.6234	3.7112	2.4281	1.7001	0.1087	0.4996
		IV	8.2936	3.7114	2.4812	1.7175	0.1129	0.4996
	Deck	I	9.1234	3.1192	0.8557	0.0000	0.0000	0.7494
		II	10.1612	2.8546	0.7010	0.0000	0.0000	0.7494
		III	8.5921	2.6382	0.6573	0.0000	0.0000	0.7494
		IV	8.2816	2.2737	0.6389	0.0000	0.0000	0.7494
Single Hull	Shell	I	6.5454	3.9808	1.5611	0.0000	0.0000	0.0000
		II	6.8927	3.8905	1.5686	0.0000	0.0000	0.0000
		III	6.1087	3.8420	1.5623	0.0000	0.0000	0.0000
		IV	5.8598	3.8408	1.5742	0.0000	0.0000	0.0000
	Deck	I	10.2789	3.7483	1.8504	0.0000	0.0000	0.0000
		II	10.9836	3.1210	1.7683	0.0000	0.0000	0.0000
		III	9.4058	4.0984	1.8702	0.0000	0.0000	0.0000
		IV	9.2576	3.3828	1.5122	0.0000	0.0000	0.0000

Table 2: Global results of proposed collision scenarios (No.* is number and Displ.** is displacement).

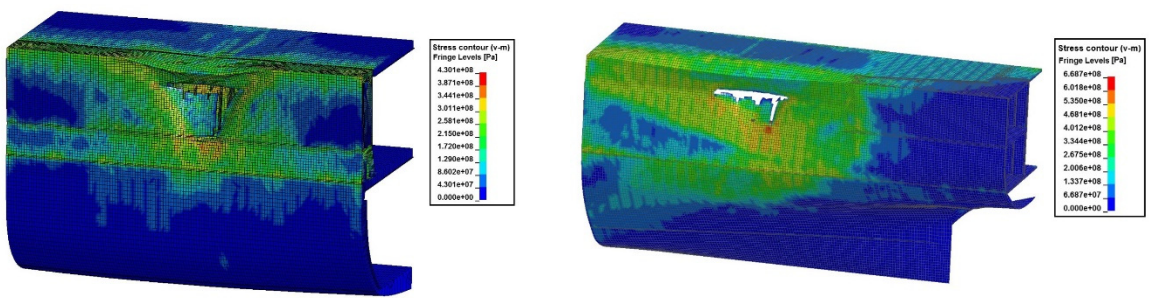

(a) (b)

Figure 4: Tearing on the outer hull during *collision to shell*: (a) the double hull and (b) the single hull. The both structures were applied by material no. II.

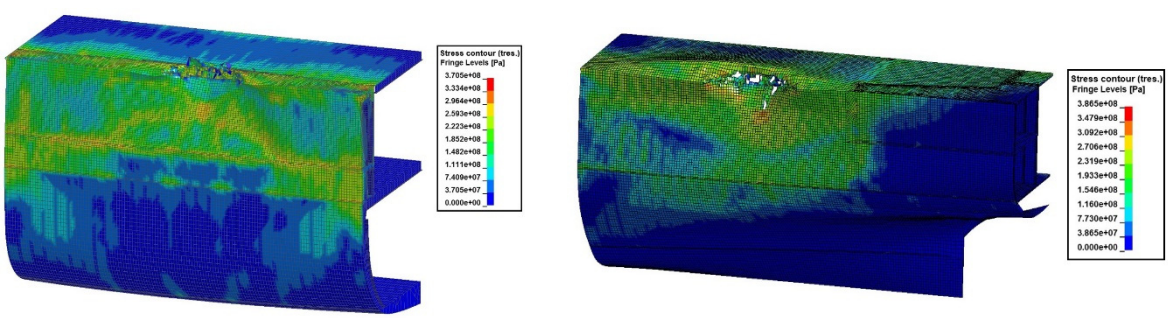

(a) (b)

Figure 5: Damage extent on the deck after collision to both structures: (a) the double hull and (b) the single hull. The both hull structures used material no. II.

In term of shear stress which is represented by the Tresca contour, distribution of the stress in the end of collision process was observed equally expanded to an area that has similar structural arrangement with the target point. On the double hull structure, the arrangement of the hull structure is similar on the entire model, including width between two hulls and frame spacing. This condition and location of the target pint which was determined almost at the middle of the struck ship made the shear stress was almost symmetrically distributed on the struck ship as presented in Figure 5a. Different tendency was shown during collision to the single hull structure. The distribution of the shear stress was asymmetric on the outer hull. This behavior took place as influenced by the geometry of the after-end structure. Compared to the double hull structure, the single hull structure was not equally arranged since in the end of model, a double hull structure was exist. In this location, the shear stress was not observed (see the end of model in Figure 5b). Model geometry and target location on the single hull structure also contributed to this phenomenon and made the stress distribution had different contour with the double hull structure.

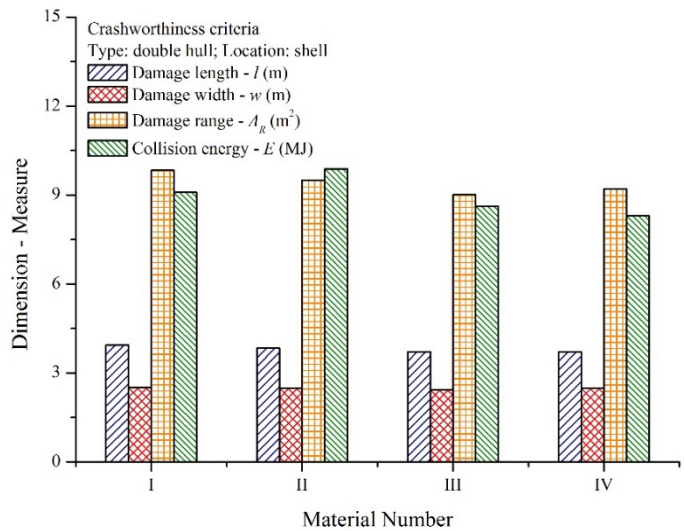

Figure 6: Comparison of the crashworthiness criteria for the double hull structure during *shell collision*.

Specific damage characteristic is discussed in order to verify the results with the previous formulae to estimate collision energy. Based on the graph in Figures 6 and 7, the damage extents of the double hull has larger range than the single hull, which the range here is the expected damaged area after collision process. This measure is obtained from calculation of damage length and width on the outer hull using fundamental area formulae $A = l * w$ where A stands for the area, l is the length and w is the width. Larger the range can be expected will produce larger collision energy. In side collision to the double and single hulls, the damage for all materials is close in term of the damage area. Nevertheless, the energy is found quite different with the material II produced the highest energy. These tendencies indicate that the inner structure such as frame and girder are highly crushed during penetration of the striking ship. It raises research opportunity which assessment of structural behaviour on the inner members subjected to collision is recommended. Despite of this difference, based on the

global crashworthiness data in Table 2, tendency of the collision energy for both hull types are considered match with the strength-energy relation during *shell collision* for all applied materials. Weaker the applied material (as found in the material I) will produce less collision energy compared to material with stronger characteristic in the material II. In the same time, structure type in the present work also shows good agreement with the produced energy level. The overall energy on the double bottom structure was found higher than the single hull type. This tendency is found consistent for all applied materials which stronger material will produce higher energy level. After double comparison in material and structural levels, it can be concluded that the strength-energy relation for material is also valid to assess resistance of a complex marine structure (i.e. single and double hulls) against collision impact.

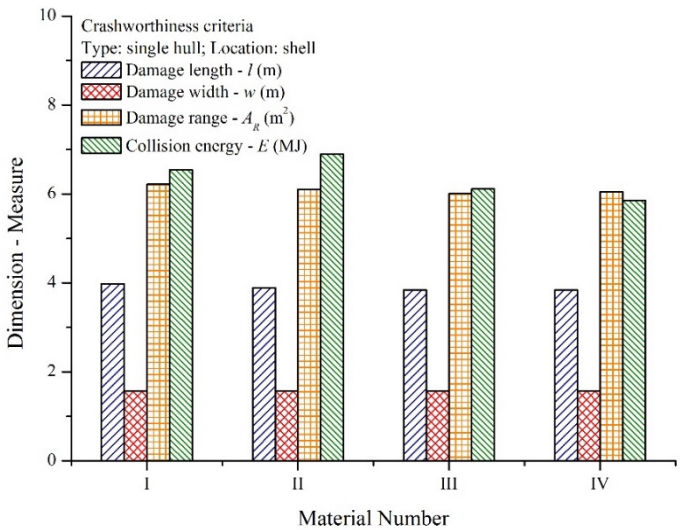

Figure 7: Comparison of the crashworthiness criteria for the single hull structure during *shell collision*.

5.3 Statistical Distribution of Damage Characteristic

A series of statistical analysis on the collision energy and damage extent is performed. Observation on deviation standard, variance of population and bell curve or as otherwise known as normal distribution analysis are presented. Several statistical data for energy and damage are presented in Figure 8. These results indicate an occurrence possibility of several crashworthiness criteria during external parameter (target location) and internal factor (structural arrangement and material type) are involved in calculation. Based on the 16 collision scenarios, the collision energy (Figure 8a) possibly occurs in range 8-11 MJ. In other hand, the produced damage length (l) and width (w) in the end of collision are found in range 3-5 m and 1-3 m consecutively. Finally, the possibility of damage range (A_R) is high in range 5-10 m^2. A statistical calculation is presented in this work in order to provide two fundamental basis in impact analysis, namely deterministic and probabilistic methodologies. The first methodology is augmented in the present work as the scenarios were defined based on the determined parameter and factor. The second one is presented in this sub-section in order to apply a concept of probabilistic method in predicting wide range impact phenomena on marine structures.

Distribution of the crashworthiness criteria can be very helpful in interpreting large amount of data and to be good method in predicting the structural behaviour and casualties after impact.

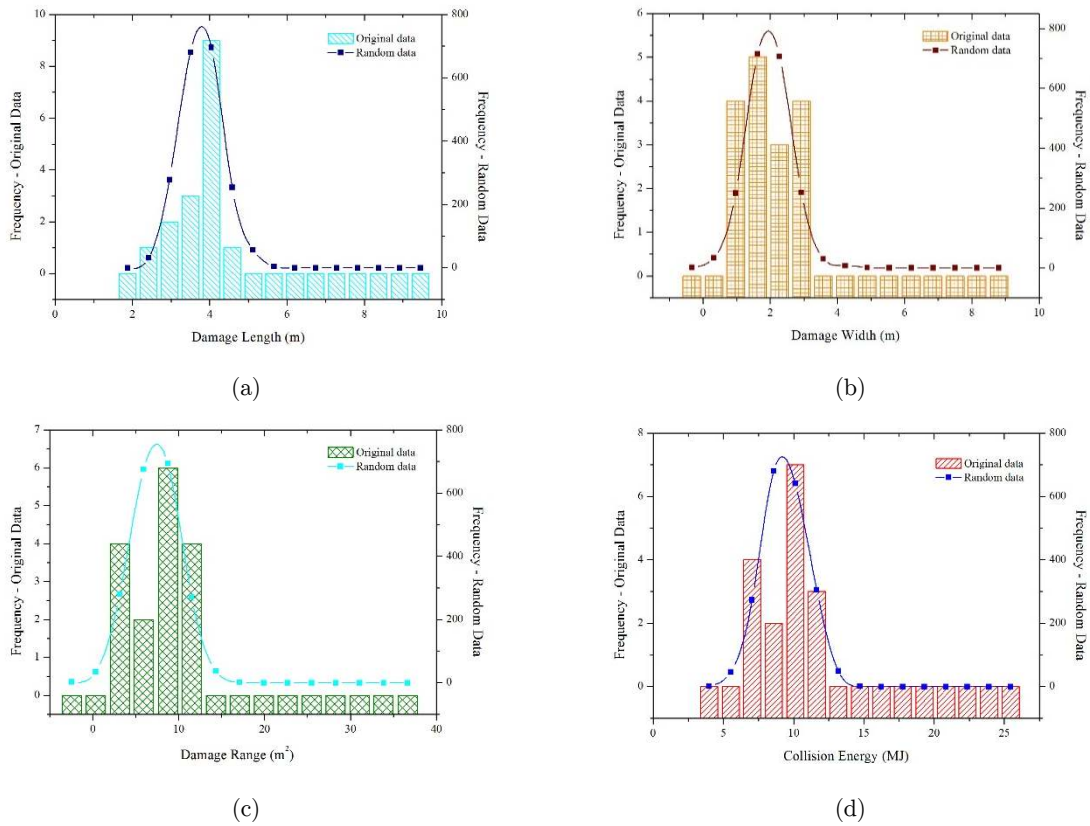

Figure 8: The bell curve analysis for the crashworthiness criteria: (a) damage length, (b) damage width, (c) damage range and (d) collision energy.

In the Appendix, the statistical data showing the damage extent of the global results. The damage of the inner hull is not presented because for the single hull structure, no inner shell was assembled and the damage did not occur in this structure. The damage on passenger cargo (vehicles since the struck ship is a Ro-Ro ship) can be predicted immense since right after failure of the outer hull, a contact between the striking ship and cargo cannot be avoided any longer for the single hull. Further assessment can be conducted in terms of survivability for passenger vessel and spillage of hazardous cargo from oil or nuclear carrier. Pioneer works are suggested, such as Alves and Oshiro (2006), Jones (2009), Ringsberg (2010) and Prabowo et al. (2017d) to be reviewed regarding development and opportunity to assess the mentioned phenomenon.

6 CONCLUSIONS

This paper presented a series of structural analysis and assessment on a maritime transportation mode, Ro-Ro passenger ship. Review of pioneer works and fundamental basis of failure formulae were

provided in the earlier part to give a solid foothold for further observation and discussion. Several collision scenarios were defined for numerical simulation to obtain the data regarding structural behaviour and crashworthiness criteria after the collision process. Numerical simulations were successfully performed by the finite element method while the analysis data was performed by direct interpretation, comparison with other method and statistical analysis. In term of structural arrangement, the single hull structure produced lesser collision energy than the double hull structure for the *shell collision*. However, similar magnitude was shown by the *deck collision* for both structural types. This energy magnitude was concluded equally perpendicular with the damage extent which is represented by the damages length and width. Verification of these results is given with empirical formulae of several pioneer works. Based on analysis of damage extent, this work presents an alternative methodology to observe overall ship crashworthiness in terms of energy and damage by observation to the damage range. It can be a useful method to reduce analysis time during verification of numerical simulation, actual experiment or impact incident is conducted using comparative study with empirical formulae. Furthermore, the statistical analysis was performed to present distribution of the collision energy and damage extent. It was successful in delivering useful information to interpret the global tendency data and estimate structural behaviour. The deviation standard, variance and bell curve analysis gave powerful enough evidence to cultivate data results for collision phenomenon.

Based on the calculation and assessment in this work, the authors conclude that the part of side hull which is not appended by the double hull structure to be the most vulnerable target against side collision impact by other ship. It is recommended during design stage, especially for hazardous carrying vessel (oil tanker and nuclear powered vessel), double hull arrangement according to Regulation 13F of Annex 1 of MARPOL is applied. Furthermore, as demand to increase safety level of passenger and cruise vessels subjected collision and grounding impacts, double hull system on side hull is also applicable for this ship type. IMO has stated in a document related to Ro-Ro safety, stability and rolling period of this ship is including in challenge of the Ro-Ro operation. In damaged condition, survivability of the ship is considered can be kept in optimum condition with double hull as sea water can be prevented to enter the main hull and influence ship stability. Overall double hull along longitudinal direction is suggested to be used rather than partial part as found in this study to avoid critical location in encountering impact phenomena. Deployments of the deterministic and probabilistic methods are highly encouraged for further analysis in field impact and failure engineering, especially for marine structures. This study can be expanded during the collision between ships is involving dual structural failure as influenced by a bulbous bow. Behaviour of the inner structures in collision can be considered as good research topic for future work.

Acknowledgement

The authors gratefully acknowledge financial support from the BK21 plus MADEC Human Resource Development Group for supporting the current work. This work was successfully carried out in *Laboratory of Ship Structure and Vibration Analysis*, Department of Naval Architecture and Marine Systems Engineering, Pukyong National University, South Korea, while preparations in material and procedure had been performed in *Laboratory of Ship Structure and Construction*, Department of Naval Architecture, Diponegoro University, Indonesia.

References

AbuBakar, A., Dow, R.S., (2013). Simulation of ship grounding damage using the finite element method. International Journal of Solids and Structures 50: 623-636.

Alsos, H.S., Amdahl, J., (2007). On the resistance of tanker bottom structures during stranding, Marine Structures 20: 218-237.

Alves, M., Oshiro, R.E., (2006). Scaling the impact of a mass on a structure, International Journal of Impact Engineering 32: 1158-1173.

ANSYS, 2017. ANSYS LS-DYNA User's Guide. ANSYS, Inc., Pennsylvania, US.

Bae, D.M., Prabowo, A.R., Cao, B., Sohn, J.M., Zakki, A.F., Wang, Q., (2016a). Numerical simulation for the collision between side structure and level ice in event of side impact scenario. Latin American Journal of Solids and Structures 13: 2691-2704.

Bae, D.M., Prabowo, A.R., Cao, B., Zakki, A.F., Haryadi, G.D., (2016b). Study on collision between two ships using selected parameter in collision simulation. Journal of Marine Science and Application 15: 63-72.

Brünig, M., Chyra, O., Albrecht, D., Driemeier, L., Alves, M., (2008). A ductile damage criterion at various stress triaxialities, International Journal of Plasticity 24: 1731-1755.

James, M.N., (2002). Crashing aircraft, sinking ships - Fractographic and SEM support for unusual hypotheses. Engineering Failure Analysis 9: 313-328.

Jones, N., (2009). Hazard assessment for extreme dynamics loading. Latin American Journal of Solids and Structures 6: 35-49.

Jones, N., Wierzbicki, T., (1983). Structural crashworthiness. Butterworth & Co. (Publishers), Ltd., Michigan, US.

Kinkead, A.N., (1980). A method for analyzing cargo protection afforded by ship structures in collision and its application to an LNG carrier. Royal Institution of Naval Architects (RINA) Transaction.

Kitamura, O., (2002). FEM approach to the simulation of collision and grounding damage. Marine Structures 15: 403-428.

Klinger, C., Bohraus, S., (2014). 1992 Northeim train crash – A root cause analysis. Engineering Failure Analysis 43: 171-185.

McDermott, J., Kline, R., Jones, E., Maniar, N., Chiang, W., (1974). Tanker structural analysis for minor collision. Society of Naval Architects and Marine Engineers (SNAME) Transaction.

Minorsky, V.U., (1958). An analysis of ship collision with reference to protection of nuclear power ships. Journal of Ship Research 3: 1-4.

Ozguc, O., Das, P.K., Barltrop, N., (2005). A comparative study on the structural integrity of single and double side skin bulk carriers under collision damage, Marine Structures 18: 511-547.

Paik, J.K., (1994). Cutting of a longitudinally stiffened plate by a wedge. Journal of Ship Research 38: 340-348.

Prabowo, A.R., Bae, D.M., Sohn, J.M., Cao, B., (2016a). Energy behavior on side structure in event of ship collision subjected to external parameters. Heliyon 2: e00192.

Prabowo, A.R., Bae, D.M., Sohn, J.M., Zakki, A.F., (2016b). Evaluating the parameter influence in the event of a ship collision based on the finite element method approach. International Journal of Technology 4: 592-602.

Prabowo, A.R., Bae, D.M., Sohn, J.M., Zakki, A.F., Cao, B., Wang, Q. (2017a). Analysis of structural behaviour during collision event accounting for bow and side structure interaction. Theoretical and Applied Mechanics Letters 7: 6-12.

Prabowo, A.R., Bae, D.M., Sohn, J.M., Zakki, A.F., Cao, B., Cho, J.H., (2017b). Effects of the rebounding of a striking ship on structural crashworthiness during ship-ship collision. Thin-Walled Structures 115: 225-239.

Prabowo, A.R., Bae, D.M., Sohn, J.M., Zakki, A.F., Cao, B., (2017c). Rapid prediction of damage on a struck ship accounting for side impact scenario models. Open Engineering 7: 91-99.

Prabowo, A.R., Bae, D.M., Sohn, J.M., Zakki, A.F., Cao, B., (2017d). Development in calculation and analysis of collision and grounding on marine structure and ocean engineering fields. Journal Aquaculture and Marine Biology 5: 00116.

Reckling, K.A., (1983). Mechanics of minor ship collisions. International Journal of Impact Engineering 1: 281-299.

Ringsberg, J.W., (2010). Characteristic of material, ship side structure response and ship survivability in ship collision. Ships and Offshore Structures 5: 51-66.

Tornqvist, R., Simonsen, B.C., (2004). Safety and structural crashworthiness of ship structures; modelling tools and application in design. International Conference on Collision and Grounding of Ships (ICCGS), Izu, Japan.

Vaughan, H., (1978) Bending and tearing of plate with application to ship-bottom damage. Journal of Naval Architects 3: 97-99.

Wang, G., Ohtsubo, H., (1997). Deformation of ship plate subjected to very large load. International Conference of Offshore, Marine and Arctic Engineering (OMAE), Yokohama, Japan.

Woisin, G., (1979). Design against collision. Schiff and Hafen 31: 1059-1069.

Zahran, M.S., Xue, P., Esa, M.S., Abdelwahab, M.M., Lu, G., (2017). A new configuration of circular stepped tubes reinforced with external stiffeners to improve energy absorption characteristics under axial impact. Latin American Journal of Solids and Structures 14: 292-311.

Zhang, S., (1999). The mechanics of ship collisions. Ph.D. Thesis, Department of Naval Architecture and Offshore Engineering, Technical University of Denmark (DTU), Lyngby, Denmark.

Zhang, X.W., Tao, Z., Zhang, Q.M., (2014). Dynamic behaviors of visco-elastic thin-walled spherical shells impact onto a rigid plate. Latin American Journal of Solids and Structures 11: 2607-2623.

APPENDIX

Arrangement Type	Target Location	Material No.*	Collision Energy	Damage Extent					
				Outer Hull			Inner Hull		
				Length	Width	Area	Length	Width	Displ.**
			(MJ)	(m)	(m)	(m^2)	(m)	(m)	(m)
Double Hull	Shell (1)	1	9.0827	3.9350	2.4994	9.8349	1.5833	0.1129	0.4996
		2	9.8800	3.8309	2.4787	9.4957	1.4605	0.1037	0.4996
		3	8.6234	3.7112	2.4281	9.0113	1.7001	0.1087	0.4996
		4	8.2936	3.7114	2.4812	9.2087	1.7175	0.1129	0.4996
	Deck (2)	1	9.1234	3.1192	0.8557	2.6690	0.0000	0.0000	0.7494
		2	10.1612	2.8546	0.7010	2.0010	0.0000	0.0000	0.7494
		3	8.5921	2.6382	0.6573	1.7341	0.0000	0.0000	0.7494
		4	8.2816	2.2737	0.6389	1.4526	0.0000	0.0000	0.7494
Mean			9.0047	3.2593	1.5925	5.6759	0.8077	0.0548	0.6245
Median			8.8531	3.4152	1.6419	5.8401	0.7303	0.0519	0.6245
Deviation Standard			0.6584	0.5844	0.8816	3.7319	0.8110	0.0548	0.1249
Variance			0.4335	0.3416	0.7772	13.9267	0.6577	0.0030	0.0156

Table A-1: Statistical data based on collision location – double hull.

Arrangement Type	Target Location	Material No.*	Collision Energy	Damage Extent					
				Outer Hull			Inner Hull		
				Length	Width	Area	Length	Width	Displ.**
			(MJ)	(m)	(m)	(m^2)	(m)	(m)	(m)
Single Hull	Shell (3)	1	6.5454	3.9808	1.5611	6.2144	0.0000	0.0000	0.0000
		2	6.8927	3.8905	1.5686	6.1025	0.0000	0.0000	0.0000
		3	6.1087	3.8420	1.5623	6.0021	0.0000	0.0000	0.0000
		4	5.8598	3.8408	1.5742	6.0463	0.0000	0.0000	0.0000
	Deck (4)	1	10.2789	3.7483	1.8504	6.9360	0.0000	0.0000	0.0000
		2	10.9836	3.1210	1.7683	5.5189	0.0000	0.0000	0.0000
		3	9.4058	4.0984	1.8702	7.6648	0.0000	0.0000	0.0000
		4	9.2576	3.3828	1.5122	5.1156	0.0000	0.0000	0.0000
Mean			8.1666	3.7381	1.6584	6.2001	0.0000	0.0000	0.0000
Median			8.0752	3.8414	1.5714	6.0744	0.0000	0.0000	0.0000
Deviation Standard			1.9017	0.3042	0.1365	0.7416	0.0000	0.0000	0.0000
Variance			3.6164	0.0926	0.0186	0.5500	0.0000	0.0000	0.0000

Table A-2: Statistical data based on collision location – single hull.